

TRANSFORMATION OF SHORT WAVES IN A NONUNIFORM FLOW FIELD ON THE OCEAN SURFACE. THE EFFECT OF WIND GROWTH RATE MODULATION

K. A. Gorshkov, I. S. Dolina, I. A. Soustova,
and Yu. I. Troitskaya

UDC 551.466.8

We develop a model of transformation of the short surface wave spectrum in the presence of a nonuniform flow on a water surface, in which the modulation of wind-wave growth rate is taken into account. The model of a turbulent near-water atmospheric layer is used to calculate the modulated growth rate. In this model, turbulent stresses in the wind are described using a gradient approximation with model eddy viscosity specified with allowance for the known laboratory experiments. The examples of short-wave modulation in the presence of nonuniform flows on a water surface, originating from ripples and intense internal waves, are considered. It is shown that deformations of the wind-velocity profile and its long-wavelength perturbation due to the nonlinear interaction between the wind surface waves and the wind has a significant effects on the short-wave growth rate and its modulation. In the case of ripples, this deformation reduces to an increase in the roughness parameter of the wind-velocity profile and to a velocity-profile modulation with ripple period. The modulated growth rate is calculated within the framework of a quasi-linear model of surface-wave generation by a turbulent wind, in which the hypothesis of random phases of the wind-wave field is used. The amplitude and phase of the hydrodynamical modulation transfer function are calculated within the framework of the relaxation model. The calculation results are in reasonable agreement with the available experimental data. A model described by the combined Korteweg – de Vries equation is used to study a surface flow field generated by intense internal waves. The internal-wave parameters are takes from the results of the COPE experiment. We calculate the wind growth-rate dependences on the wave-train phase for the cases of downwind and upwind propagation of an internal wave. The calculation results agree qualitatively with experimental data.

1. INTRODUCTION

One of the most prospective methods for remote studying of the ocean is based on measuring variations in the radar signals scattered by a rough water surface. Variations in the received signal originate from the variability of wind-roughness parameters, which, in turn, results from transformation of these parameters in the field of nonuniform large-scale flows on the surface. Such flows are caused by various processes in the upper layer of the ocean, e.g., internal waves, flows around islands and underwater eminences, etc. Typical scales of such flows amount to hundreds of meters. Long surface waves, including ripples, can have similar scales. The variability due to such large-scale flows are observed over the wide wind-roughness spectrum comprising wavelengths from a few meters to a few centimeters. Modulation of the amplitude of a decimeter wave in a field of internal waves and nonuniform flows is well explained within the framework of the kinematic mechanism [1]. At the same time, the mechanism of centimeter-wave modulation is not clarified completely, despite the rapt attention to this surface-wave band which determines sea-surface radio images

Institute of Applied Physics of the Russian Academy of Sciences, Nizhny Novgorod, Russia. Translated from *Izvestiya Vysshikh Uchebnykh Zavedenii, Radiofizika*, Vol. 46, No. 7, pp. 513–536, July, 2003. Original article submitted June 6, 2003.

formed by the Bragg mechanism. A hypothesis on the “cascade mechanism” of centimeter-wave modulation was put forward in the middle of the eighties [2]. A physical explanation for the cascade mechanism, proposed recently, treats it as a modulation of the stimulated higher harmonics of decimeter waves [3]. However, it should be noted that, according to experiments, stimulated decimeter-wave harmonics significantly contribute to the centimeter wave-roughness spectrum under conditions of a strong wind [3]. In addition, we should note that if waves with steep crests exist on a water surface, the radio-wave scattering can be determined by scattering from such crests. In this case, the wavelengths of surface and radio waves are not related by the resonance Bragg condition [4], and the decimeter surface waves can efficiently scatter the centimeter radio waves. However, this mechanism becomes efficient only if the wind is sufficiently strong and the major fraction of wind waves have steep crests.

If a wind is weak, then waves have flat profiles, and the surface roughness is mainly contributed by free wind-excited waves. In this case, variations in the wind-velocity profile due to a nonuniform flow on the water surface modulate the short-wave growth rate. Such modulation can notably influence the variability of the spectrum of centimeter surface waves. The effect of wind growth-rate modulation is now actively discussed in relation to the problem of determination of the hydrodynamical modulation transfer function (MTF) of long surface waves and ripples [5–9]. In addition, the influence of this effect on the centimeter-wave modulation in the field of intense internal waves is discussed at present [10].

In this paper, we present a theoretical model for the mechanism of modulation of the growth rate of short surface waves in the presence of nonuniform flows and discuss applications of this model to observations of the surface-wave modulation in the presence of ripple waves or intense internal waves. Basic equations describing transformation of the spectrum of short surface waves in the presence of nonuniform flows on a water surface are given in Sec. 2. Basic equations describing a wind turbulent boundary layer above a rough water surface are given in Sec. 3. The hydrodynamical MTF of ripple waves is found in Sec. 4 in which our model is also compared with the available experimental data. A model of centimeter-wave modulation in a field of intense internal waves is described in Sec. 5. Here, the calculations are also compared with data of the COPE experiment [11].

2. BASIC EQUATIONS DESCRIBING MODULATION OF THE SPECTRUM OF SHORT SURFACE WAVES IN THE PRESENCE OF NONUNIFORM FLOWS ON A WATER SURFACE

Short-wave modulation in a field of nonuniform flows is described by the kinetic equation for the short-wave elevation spectrum $F(K, x, t)$. In the simplest case where the directions of wind, waves, and flow are identical and the modulation is maximum, this equation reads

$$\frac{\partial F}{\partial t} + [U_0(x, t) + C_{\text{gr}}] \frac{\partial F}{\partial x} - \frac{\partial \Omega}{\partial x} \frac{\partial F}{\partial K} = 2B[F, K, U, x, t] + \tilde{\eta} \frac{\partial U_0}{\partial x} F + \text{Int}[F, K]. \quad (1)$$

Here, $U_0(x, t)$ is the nonuniform flow field, K and Ω are the wavenumber and frequency of the short wave in the laboratory frame, $\Omega = KU_0(x, t) + \Omega_0$, Ω_0 is the short-wave eigenfrequency, $B[F, K, U, x, t]$ is the modulated short-wave growth rate equal to the algebraic sum of the wind growth rate, determined by the wind velocity U , and the viscous decay rate (this term depends on the long-wave field), $\text{Int}[F, K]$ is the “collision integral” describing the nonlinear wave interaction. The second term on the the right-hand side stands for the radiative stress, while $\tilde{\eta}$ is the factor introduced in [12–14]. Note that the equation for the wave-action spectrum \tilde{N} does not comprise the radiative stress. In this case, an expression for $\tilde{\eta}$ can readily be obtained from the relationships between the spectra \tilde{N} and F of the wave action and elevation, respectively, i.e., $\tilde{\eta}$ is determined by the dispersion characteristics of the waves.

For potential waves in the absence of a drift flow we have

$$\tilde{\eta} = C_{\text{gr}}/C_{\text{f}} - 1,$$

where $C_{\text{gr}} = \partial\Omega_0/\partial K$ and $C_{\text{f}} = \Omega_0/K$ are the group and phase velocities of the short wave, respectively.

If a nonuniform flow on a water surface is sufficiently weak and the variations in the short-wave spectrum originating from this flow are small, then the collision integral $\text{Int}[F, K]$ in Eq. (1) can be approximated by the relaxation model proposed in [15].

Let the equilibrium spectrum F_0 of the elevations of a rough water surface for the wind velocity U obeys the equation

$$2B[F_0, K, U]F_0 + \text{Int}[F_0, K] = 0$$

following from Eq. (1).

Similar to [15], we consider the spatially uniform small perturbation F_1 of the elevation spectrum:

$$F = F_0[K] + F_1[F_0, \mathbf{k}, t].$$

Such a perturbed spectrum relaxes to the equilibrium spectrum. If β_r denotes the relaxation rate, then

$$F_1[F_0, \mathbf{k}, t] = F_1 \exp(-\beta_r t),$$

while Eq. (1) in the linear approximation with respect to F_1 yields

$$-\beta_r F_1 = \frac{\partial F_1}{\partial t} = \left(\frac{\delta}{\delta F} \text{Int}[F] \Big|_{F=F_0} + 2B[F_0, K, U] + 2 \frac{\delta B_0}{\delta F} \Big|_{F=F_0} F_0 \right) F_1,$$

where $\delta/\delta F$ denotes the variational derivative. Then the variational derivative of the collision integral is

$$\frac{\delta}{\delta F} \text{Int}[F, K] \Big|_{F=F_0[K]} = - \left(2B_0[F_0, K, U] + 2 \frac{\delta B_0}{\delta F} \Big|_{F=F_0[K]} F_0 + \beta_r \right). \quad (2)$$

As in [15], the approximation of the collision integral is also used in the case where the spectrum perturbation is a function of the spatial coordinate. Assume that a perturbation of the short-wave spectrum is caused by a nonuniform flow on a water surface, then transformation of short waves in the field of this nonuniform flow and wind growth rate modulation are the mechanisms sustaining this perturbation. In this case, modulation of the amplitude-dependent wind growth rate of the short waves are determined by two factors: perturbations of the wind velocity, induced by the nonuniform flow, and modulation of the wind-wave amplitude, i.e.,

$$B[F, K, U, x, t] = B_0[F_0, K, U] + \frac{\delta B_0}{\delta U} U_1(x, t) + \frac{\delta B_0}{\delta F} F_1(x, t),$$

where $U_1(x, t)$ is the wind-velocity perturbation due to the nonuniform flow. If the nonuniform flow is sufficiently slow, so that long-wavelength variations in the wind velocity are determined by variations in the tangential stress T whose unperturbed value is equal to u_*^2 , then

$$B_1 = \frac{\delta B_0}{\delta u_*^2} T_1 + \frac{\delta B_0}{\delta F} F_1, \quad (3)$$

where T_1 is the long-wavelength perturbation of the tangential stress.

Substituting the formula for B into Eq. (1) and taking into account Eq. (3) for B_1 and Eq. (2) for the variation in the collision integral, we obtain in the linear approximation the following equation for F_1 :

$$\frac{\partial F_1}{\partial t} - K \frac{\partial F_0}{\partial K} \frac{\partial U_0}{\partial x} = -\beta_r F_1 + \tilde{\eta} \frac{\partial U_0}{\partial x} F_0 + 2 \frac{\delta B_0}{\delta T} \Big|_{T=u_*^2} T_1 F_0.$$

If the nonuniform flow is a small-amplitude harmonic wave with the elevation

$$\eta = a \cos(\omega t - kx), \quad (4)$$

then

$$U_0 = cka \exp[i(kx - \omega t)], \quad F_1 = F_{10} \exp[i(kx - \omega t)]$$

and

$$F_1 = \frac{i\omega ka}{\beta_r - i\omega} \left(K \frac{\partial F_0}{\partial k} + \tilde{\eta} F_0 \right) + 2 \frac{\delta B_0}{\delta u_*^2} T_1 \frac{F_0}{\beta_r - i\omega}, \quad (5)$$

where c is the phase velocity of the wave. In what follows, similar to [15], we put the relaxation rate equal to $2B_0[F]$.

The first term in Eq. (5) describes conservative transformation of short waves in a nonuniform flow field. Estimates show that this mechanism dominates modulation of the decimeter waves in the presence of internal waves [1, 2] and is very important for the formation of the hydrodynamical MTF of long surface waves [16]. At the same time, it is important to infer additional factors to explain the centimeter-wave modulation in the presence of both internal and long surface waves. The second term in Eq. (5) describes the effect of wind growth rate modulation of surface waves, which is discussed in this paper. Calculation of this growth rate requires a model of the wind boundary layer above a rough water surface.

3. WIND BOUNDARY LAYER ABOVE A WATER SURFACE WITH A NONUNIFORM FLOW FIELD

Consider a wind boundary layer above a water surface. To describe average fields, we apply the system of Reynolds equations [17] based on the simplest closure hypothesis consisting in a gradient approximation of turbulent stresses:

$$\sigma_{ij} = -\frac{2}{3} \langle u_i'^2 \rangle \delta_{ij} + \nu \left(\frac{\partial \langle u_i \rangle}{\partial x_j} + \frac{\partial \langle u_j \rangle}{\partial x_i} \right). \quad (6)$$

Here, $\langle u_i \rangle$ is the i th component of the average velocity, $\langle u_i'^2 \rangle$ is the average kinetic energy of turbulent pulsations, ν is the turbulent viscosity coefficient, and δ_{ij} is the Kronecker delta. Let ν be a given function of the vertical coordinate z . The following approximation obtained in [18] is a good representation of the function $\nu(z)$:

$$\nu(z) = \nu_a [N_0 + 0.4z^+ (1 - \exp[-(z^+/L)^2])]. \quad (7)$$

Here, $z^+ = zu_*/\nu_a$ is the vertical coordinate in the units of the viscous length, u_* is the wind friction velocity, and ν_a is the kinematic viscosity of the air. The parameters L and N_0 in Eq. (7) are determined by the regime of flow over the surface. In the case of hydrodynamically smooth flow over a water surface, $L = 22.4$ and $N_0 = 1$. The influence of the water-surface roughness due to the existence of waves on the surface can be taken into account by solving the problem of momentum transfer from the wind to the waves, which is done in Sec. 4. Another simplified method was proposed in [19], which yields $N_0 > 1$ for a rough surface. This method is used in Sec. 5. Note that Eq. (7) describes the effective viscosity in both the viscous sublayer and in the logarithmic boundary layer.

Let us consider two-dimensional motions for which the system of Reynolds equations can be written for the vorticity χ and the stream function ψ :

$$\frac{\partial \chi}{\partial t} + \frac{\partial \psi}{\partial z} \frac{\partial \chi}{\partial x} - \frac{\partial \psi}{\partial x} \frac{\partial \chi}{\partial z} - \Delta(\nu \chi) + 2 \frac{\partial^2 \nu}{\partial z^2} \frac{\partial^2 \psi}{\partial x^2} = 0, \quad \Delta \psi = \chi. \quad (8)$$

The boundary conditions of impenetrability and adherence,

$$\frac{\partial \zeta}{\partial t} + \frac{\partial \psi}{\partial z} \frac{\partial \zeta}{\partial x} + \frac{\partial \psi}{\partial x} \Big|_{z=\zeta(x,t)} = 0, \quad \frac{\partial \psi}{\partial z} \Big|_{z=\zeta(x,t)} = \frac{\partial \psi_w}{\partial z} \Big|_{z=\zeta(x,t)}, \quad (9)$$

where ψ_w is the stream function of the flow in the water, hold on the water surface $z = \zeta(x, t)$.

The considered model of a near-water atmospheric boundary layer takes into account a viscous sublayer of an extremely small thickness no larger than 1 mm, which is much less than the typical surface-wave

height. Hence, to exclude the strong geometrical nonlinearity, one should use curvilinear coordinates such that one coordinate line coincides with the rough water surface [20]. In the case of orthogonal coordinates (s, γ) specified by the transformation

$$x = x(s, \gamma, t), \quad z = z(s, \gamma, t),$$

where $z = z(s, \gamma = 0, t)$ is the water-surface equation, system (8) takes the form [21]

$$\begin{aligned} & \chi_t + \frac{\chi_s}{I} [\psi_\gamma - (x_s x_t + z_s z_t)] - \frac{\chi_\gamma}{I} [\psi_s + (x_\gamma x_t + z_\gamma z_t)] = \\ & = \frac{\Delta(\nu\chi)}{I} - \frac{2}{I^2} \nu_{\gamma\gamma} \psi_{ss} - \frac{I_\gamma}{I^3} [(\psi_\gamma \nu_\gamma)_\gamma - \nu_\gamma \psi_{ss}] - \frac{I_s}{I^3} (2\nu_\gamma \psi_{s\gamma} - \psi_s \nu_{\gamma\gamma}) + \psi_\gamma \nu_\gamma \frac{I_s^2 + I_\gamma^2}{I^4}, \end{aligned} \quad (10a)$$

$$\Delta\psi = \chi = \frac{\psi_{ss} + \psi_{\gamma\gamma}}{I}, \quad (10b)$$

while boundary conditions (9) take the form

$$\psi|_{\gamma=0} = 0, \quad (10c)$$

$$\frac{\partial\psi}{\partial\gamma} \frac{1}{\sqrt{I_a}} = \frac{\partial\psi_w}{\partial\gamma} \frac{1}{\sqrt{I_w}}. \quad (10d)$$

Hereafter, the subscript denotes the partial derivative over the corresponding coordinate, $I = \partial(x, z)/\partial(s, \gamma)$ is the Jacobian of the orthogonal coordinate transformation, and the subscripts ‘‘a’’ and ‘‘w’’ refer to the corresponding quantities in the air and water, respectively.

Within the framework of the proposed model, the modulated wind-wave growth rate can be found in a fairly simple way if the typical temporal and spatial scales, τ and λ , of the surface waves are small compared with the corresponding flow scales T_0 and L_0 , i.e., if there exists the small parameter $\mu = 0(\tau/T_0, \lambda/L_0)$ of the problem. In this case, the problem is solved as follows. At first, the variable flow of the wind, which is induced in the air by a flow on a water surface, is found within the framework of the model described by Eqs. (10a), (10b), and (11). Next, the wind growth rate of sufficiently short surface waves in the lowest order of μ , which corresponds to the parametric approximation, is obtained. In what follows we present the examples of calculations of the modulated growth rate of short surface waves and modulation of their spectral density for two cases, namely, ripple waves and intense internal waves.

4. MODULATION OF WIND WAVES BY RIPPLE WAVES

It was shown above that modulation of the short-wave spectrum in the presence of ripple waves is described by Eq. (5) which comprises the complex amplitude of the long-wavelength perturbation of the short-wave growth rate $T_1(\delta B_0/\delta T)|_{T=u_*^*}$, where T_1 is the complex amplitude of the long-wavelength perturbation of the tangential turbulent stress of the wind. Let us calculate this quantity within the framework of the adopted model. The problem splits into two: (i) determination of the long-wavelength perturbation of the wind velocity, which is induced by a ripple and (ii) determination of the short-wavelength perturbation.

4.1. Average flow and long-wavelength perturbation

Under oceanic conditions, the elevation of a water surface in a ripple waves is much larger than the thickness of the viscous sublayer of the atmospheric boundary layer even if the ripple-wave amplitude is small. Therefore, we firstly apply the transformation to the curvilinear coordinate system (s, γ) in which one coordinate line coincides with the water surface perturbed by a long wave. In the case of a harmonic wave with elevation field (4) the curvilinear coordinates in the reference frame moving with phase velocity of the long wave are time-independent:

$$x = s - a \exp(-k\gamma) \sin(ks), \quad y = \gamma + a \exp(-k\gamma) \cos(ks).$$

Thus, the system of hydrodynamical equations in terms of the vorticity and stream function is identical to Eqs. (10a) and (10b) if $x_t = y_t = 0$.

The solution of Eqs. (10a) and (10b) can be represented as the sum of the stream function ψ_0 and vorticity χ_0 averaged over the wave perturbations, the long-wavelength perturbations $\psi^{(l)}$ and $\chi^{(l)}$ of these quantities, induced by a ripple wave with elevation (4), and the short-wavelength perturbations $\psi^{(s)}$ and $\chi^{(s)}$ due to wind waves. Hence,

$$\psi = \psi_0(\gamma) + \psi^{(l)}(\gamma, s) + \psi^{(s)}(\gamma, s, t), \quad \chi = \chi_0(\gamma) + \chi^{(l)}(\gamma, s) + \chi^{(s)}(\gamma, s, t)$$

in the reference frame moving with phase velocity of the wave.

It is well known that wave perturbations decrease at distances from the surface exceeding about the corresponding wavelength. We will consider such distances for which the short-wavelength perturbations are small compared with the long-wavelength ones.

Averaging the system of Eqs. (10a) and (10b) over the short-wavelength perturbations and linearizing the resulting equations with respect to the long-wavelength perturbations, we obtain

$$\frac{d^2}{d\gamma^2}(\nu\chi_0) + \frac{d^2}{d\gamma^2}\Sigma_0(\gamma) = 0, \quad (11)$$

$$\psi_{0\gamma\gamma} = \chi_0, \quad (11)$$

for the average flow and

$$\frac{\partial\chi^{(l)}}{\partial s} \frac{\partial\psi_0}{\partial\gamma} - \frac{\partial\chi_0}{\partial\gamma} \frac{\partial\psi^{(l)}}{\partial s} - \left[\frac{\partial^2}{\partial\gamma^2} + \frac{\partial^2}{\partial s^2} \right] \nu\chi^{(l)} = \frac{\partial^2[\Sigma_1(\gamma, s) - 2y_{1\gamma}\Sigma_0(\gamma)]}{\partial\gamma^2} - 2\nu_{\gamma\gamma}\psi_{ss}^{(l)} - I_\gamma(\nu_\gamma\psi_{0\gamma}), \quad (12a)$$

$$\frac{\partial^2\psi^{(l)}}{\partial\gamma^2} + \frac{\partial^2\psi^{(l)}}{\partial s^2} = \chi^{(l)} + 2y_{1\gamma}\chi_0 \quad (12b)$$

for the long-wavelength perturbation. Here, $\Sigma_0(\gamma)$ and $\Sigma_1(\gamma, s)$ are the average value and the long-wavelength perturbation of the wind-wave momentum flux:

$$\Sigma_0(\gamma) + \Sigma_1(\gamma, s) \approx -\frac{\partial^2}{\partial\gamma^2} \overline{\psi_\gamma^{(s)}\psi_s^{(s)}}, \quad (13)$$

where the overbar denotes averaging over short-wavelength perturbations. Since $\psi^{(s)}$ decreases with distance from the air–water interface, it is evident from Eq. (13) that the wave momentum flux Σ decreases, as well. In this case, as was shown in [22], the wave momentum flux for wind waves, whose phase velocities are, by definition, less than $20u_*$, undergoes significant variations in the vicinity of the surface in the transition region from the viscous sublayer to the logarithmic boundary layer, i.e., the scale δ of variation in the quantities Σ_0 and Σ_1 amounts to 20–30 viscous lengths ν_a/u_* .

As the distance from the surface increases, the average vorticity field obeys the boundary condition

$$\nu\chi_0|_{\gamma\rightarrow\infty} = u_*^2, \quad (14)$$

while long-wavelength perturbations decrease:

$$\{\psi^{(l)}, \chi^{(l)}\}|_{\gamma\rightarrow\infty} \rightarrow 0. \quad (15)$$

If the characteristic scale of the long-wave boundary layer is small compared with its wavelength, while the phase velocity is large compared with the flow velocity inside the boundary layer, then Eqs. (12a) and (12b) reduce to one equation for the long-wavelength perturbation of the turbulent stress, which, by applying the gradient approximation of turbulent stresses, can be presented in the following form:

$$T^{(1)} = \nu\chi^{(1)}, \quad (16)$$

$$\frac{\partial^2 T^{(1)}}{\partial \gamma^2} + ikc\chi^{(1)} = -\frac{\partial^2}{\partial \gamma^2} [\Sigma_1(\gamma) - 2y_{1\gamma}\Sigma_0(\gamma)], \quad (17)$$

$$\frac{\partial^2 \psi^{(1)}}{\partial \gamma^2} = \chi^{(1)}.$$

The typical vertical scale of the long-wavelength perturbation of the turbulent stress $T^{(1)}$ is equal to $L_T \approx \kappa u_*/(ck) \ll 1/k$ since $u_*/c \ll 1$, where $\kappa = 0.4$ is the Carman constant.

Equation (17) can be solved by the technique of matched asymptotic expansions if the scale L_T is much larger than the scale $\delta = (20-30)\nu_a/u_*$ of the sources on the right-hand sides of Eqs. (12a) and (12b). This condition can be written as $ck \ll u_*^2/(30\nu_a)$. For the threshold friction speed $u_* \approx 5$ cm/s of a wind, for which generation of the waves takes place [21], and the air viscosity $\nu_a = 0.15$ cm²/s, the frequency of ripple waves should be much less than 6 s⁻¹, which is valid for almost all cases.

If the conditions $\delta \ll \gamma \ll k^{-1}$ are satisfied, then the terms on the right-hand sides of Eqs. (12a) and (12b) are negligibly small and the eddy-viscosity coefficient in this region is equal to $\nu = \kappa u_* \gamma$. Then Eq. (17) yields the equation

$$\frac{d}{d\gamma} \gamma \frac{dU^{(1)}}{d\gamma} + \frac{ikc}{\kappa u_*} U^{(1)} = 0, \quad (18)$$

$$U^{(1)}|_{\gamma \rightarrow \infty} = 0 \quad (19)$$

for the long-wavelength perturbation $U^{(1)}$ of the wind velocity, which is related to $T^{(1)}$ as follows: $T^{(1)} = \kappa u_* \gamma \partial U^{(1)} / \partial \gamma$.

The solution of Eq. (18), which decreases with increasing distance from the surface, can be expressed in terms of modified Bessel functions:

$$U^{(1)} = BK_0 \left(2 \exp(i\pi/4) \sqrt{\gamma^+ ck\nu_a/u_*^2} \right), \quad (20)$$

where $\gamma^+ = \gamma u_*/\nu_a$.

A modified Bessel function has the logarithmic asymptotic

$$U^{(1)} = \frac{T_1}{\kappa u_*} \left[\ln \left(\frac{3.15kc\nu_a}{u_*^2} \gamma^+ \right) + \frac{\pi i}{2} \right] \quad (21)$$

for $\gamma^+ ck\nu_a/u_*^2 \ll 1$. It follows from Eq. (21) that the long-wavelength perturbations of the tangential stress tend to the constant value $T^{(1)} = T_1$ in this case. The unknown constant T_1 can be found using the conditions of matching the obtained “external” solution, valid at large distances from the surface, with the “internal” solution which holds near the surface.

4.2. Short-wavelength perturbation

For simplicity, we consider here only waves with wavevectors directed downwind. Actually, the wavevectors of wind waves can be directed arbitrarily, so that the model presented here can only be considered an estimation model aimed at illustrating how the nonlinear effects, caused by interaction of the waves with a wind, influence the transformation of the short-wave spectrum.

4.2.1. Short-wavelength perturbation in the “long-wavelength” coordinates (s_1, γ)

In the zeroth order with respect to the small parameter μ of the problem, the equations describing short waves against the background of a field of long waves can be written as follows [9]:

$$\begin{aligned} \frac{\partial(XI)}{\partial t} + \frac{\partial X}{\partial s_1} \frac{\partial \Phi}{\partial \gamma} - \frac{\partial X}{\partial \gamma} \frac{\partial \Phi}{\partial s_1} &= I \Delta(\nu X) - 2I\nu_{\gamma\gamma} \frac{\partial^2 \Phi}{\partial s_1^2}, \\ \left(\frac{\partial^2}{\partial \gamma^2} + \frac{\partial^2}{\partial s_1^2} \right) \Phi &= IX. \end{aligned} \quad (22)$$

System (22) is written in the coordinates (s_1, γ) , where $s_1 = s + ct$ and

$$\begin{aligned} \Phi &= \psi + cI\gamma = \int_0^\gamma U_0(\gamma_1) d\gamma_1 + \text{Re} \left[(\psi^{(1)}(\gamma) - 2kac\gamma) \exp[ik(s_1 - ct)] \right] + \psi^{(s)}(s_1, \gamma, t) \\ &= \Phi_0(\gamma, \Sigma) + \psi^{(s)}(s_1, \gamma, t). \end{aligned} \quad (23)$$

The functions Φ and X approximate the stream function and vorticity in the coordinates (s_1, γ) and $\Sigma = ik(s_1 - ct)$ is the “slow” coordinate (with respect to the short-wavelength perturbations) reckoned along the surface perturbed by the long-wavelength wave.

Let us present the field of surface elevations in the form of the Fourier–Stieltjes integral

$$\xi(s_1, \gamma, t) = \int dA(K) \exp[i(Ks - \Omega(K)t)].$$

Assume for simplicity that the phases of the short-wavelength field are random, then

$$dA(K) dA(K_1) = F_0(K) \delta(K - K_1) dK dK_1, \quad (24)$$

where $F_0(K)$ is the equilibrium spectrum of water-surface heights.

If the wave spectrum is sufficiently wide, then the problem can be solved in the quasi-linear approximation analogous to the one used in the theory of interaction of waves and particles in a plasma [23]. Within the framework of the quasi-linear approximation, the equations for each harmonic are linear, while the nonlinearity affects only the average fields of velocity, vorticity, etc.

4.2.2. Short-wavelength perturbation in the “short-wavelength” coordinates (ξ, η) “adapted” for the random field of short waves

The wave field in the quasi-linear approximation should be sought as the sum of independent harmonics. The displacement of the water surface due to the wind-wave field can be large in comparison with the thickness of the viscous sublayer in the air. To avoid this geometrical nonlinearity, we use, as in [24], the curvilinear coordinates such that one coordinate line coincides with the water surface in the first approximation with respect to the surface-height amplitude. Let us apply the following coordinate transformation:

$$\begin{aligned} s_1 &= \xi + \int_{-\infty}^{+\infty} i \exp[iK(\xi - \Omega(K)t/K) - K\eta + i\varphi_K] dA, \\ \gamma &= \eta + \int_{-\infty}^{+\infty} \exp[iK(\xi - \Omega(K)t/K) - K\eta + i\varphi_K] dA, \end{aligned} \quad (25)$$

where $\Omega(K)/K$ is the phase velocity of the K th harmonic and φ_K is the phase of this harmonic, which is assumed random.

Similar to [24], the expression for the stream function is written in the following form:

$$\Phi = \Phi_0(\eta, \Sigma) + \varphi^{(s)}(\xi, \eta, t). \quad (26)$$

Equations (23) and (26) comprise the same function Φ_0 describing the average flow and its long-wavelength perturbation. However, this function in Eq. (26) is equal to η and not to γ . In this case, the short-wavelength perturbation $\varphi^{(s)}(\xi, \gamma, t)$ of the stream function, which enters Eq. (26), differs from the term $\psi^{(s)}(s_1, \gamma, t)$ in Eq. (23) since the former function describes the stream-line deviation from the coordinate lines given by Eq. (25).

The stream function Φ and the vorticity X obey the system of equations

$$J^3 I \left[\frac{\partial \chi}{\partial t} - \frac{\partial \chi}{\partial \xi} \frac{s_{1t} s_{1\xi} + \gamma_{1t} \gamma_{1\xi}}{J} - \frac{\partial \chi}{\partial \eta} \frac{s_{1t} s_{1\eta} + \gamma_{1t} \gamma_{1\eta}}{J} \right] + J^2 \left(\frac{\partial X}{\partial \xi} \frac{\partial \Phi}{\partial \eta} - \frac{\partial X}{\partial \eta} \frac{\partial \Phi}{\partial \xi} - \left(\frac{\partial^2}{\partial \xi^2} + \frac{\partial^2}{\partial \eta^2} \right) (\nu X) \right) = -2\nu_{\eta\eta} \Phi_{\xi\xi} J - J_{\eta} [(\nu_{\eta} \Phi_{\eta})_{\eta} + \nu_{\eta} \Phi_{\xi\xi}] - J_{\xi} (2\nu_{\eta} \Phi_{\xi\eta} - \Phi_{\xi} \nu_{\eta\eta}) + \nu_{\eta} \Phi_{\eta} \frac{J_{\xi}^2 + J_{\eta}^2}{J}, \quad (27a)$$

$$\left(\frac{\partial^2}{\partial \xi^2} + \frac{\partial^2}{\partial \eta^2} \right) \Phi = I J X, \quad (27b)$$

where $J = (s_{1\xi})^2 + (s_{1\eta})^2$. This system results from system (22) upon coordinate transformation (25). The boundary conditions for system (27) are as follows [9]:

$$\Phi|_{\eta=0} = 0 \quad (27c)$$

is the condition of impenetrability of the water surface,

$$\Phi_{\eta}|_{\eta=0} = (1 + 2y_{\gamma}) \int 2\Omega \, dA \quad (27d)$$

is the condition of adherence on the water surface, and

$$\nu X|_{\eta \rightarrow \infty} = u_*^2 + \text{Re}[T_1 \exp(i\Sigma)] \quad (27e)$$

is the condition ensuring the vorticity-field matching with the external solution and the decrease in the short-wavelength perturbations.

The wave perturbations

$$\left\{ \begin{array}{l} \varphi^{(s)} \\ \chi^{(s)} \end{array} \right\} = \int_{-\infty}^{+\infty} \exp[iK(\xi - \Omega(K)t/K)] \left\{ \begin{array}{l} \Phi_2(\eta) \\ X_2(\eta) \end{array} \right\} dA(K)$$

in the quasi-linear approximation obey the system

$$\begin{aligned} (1 + 2y_{1\gamma}) [(\Phi_{0\eta} - \Omega/K) X_2 - \Phi_2 X_{0\eta}] iK \\ = (1 + 2y_{1\gamma}) (d^2/d\eta^2 - K^2) (\nu X_2) + 2K^2 \Phi_2 \nu_{\eta\eta} - 2K \exp(-K\eta) [\nu_{\eta} (\Phi_{0\eta} - \Omega/K)]_{\eta}, \\ \Phi_{2\eta\eta} - K^2 \Phi_2 = [X_2 - 2K \exp(-K\eta) X_0] (1 + 2y_{1\gamma}) \end{aligned} \quad (28)$$

of linear equations, following from Eqs. (27a) and (27b), with boundary conditions on the surface:

$$\Phi_2|_{\eta=0} = 0, \quad \Phi_{2\eta}|_{\eta=0} = (1 + 2y_{\gamma}) 2\Omega(K),$$

following from Eqs. (27c) and (27d) and complemented by the condition that the perturbations vanish at infinity.

In turn, the average values $\Phi_{0\eta}$ and X_0 obey the system of equations

$$\frac{d^2}{d\eta^2}(\nu X_0) = \frac{d^2}{d\eta^2}[\tau_{\text{wave}}(\eta)], \quad (29a)$$

$$\frac{d^2\Phi_0}{d\eta^2} = \left[X_0 \left(1 + \int_{-\infty}^{+\infty} F_0(K) K^2 \exp(-2K\eta) dK \right) + 2 \int_{-\infty}^{+\infty} \text{Re}(X_2 F_0(K) K^2 \exp(-K\eta)) dK \right] (1 + 2y_{1\gamma}), \quad (29b)$$

which can be obtained by averaging Eqs. (27a) and (27b) over the coordinate ξ . Here, $F_0(K)$ is the spectrum of water-surface elevations in Eq. (24) and

$$\tau_{\text{wave}} = \int_0^\eta K d\tilde{\eta} \left[-\frac{1}{2} \text{Im}[\Phi_2^* X_2 F_0(K)] dK + \int_{-\infty}^{+\infty} [\exp(-K\tilde{\eta}) \nu_{\tilde{\eta}} \text{Re}(\Phi_{2\tilde{\eta}} - K\Phi_2) + 2 \exp(-2K\tilde{\eta}) \nu_{\tilde{\eta}} \Phi_{0\tilde{\eta}}] F_0(K) K^2 dK \right]$$

has the meaning of the momentum flux from the waves to the wind, averaged over the horizontal coordinate ξ .

The boundary conditions

$$\Phi_{0\eta}|_{\eta=0} = 0, \quad (29c)$$

$$\nu X_{0\eta}|_{\eta \rightarrow \infty} = u_*^2 + \text{Re}[T_1 \exp(i\Sigma)] \quad (29d)$$

for the system of Eqs. (29a) and (29b) follow from Eqs. (27d) and (27e). Integrating the system of Eqs. (29a) and (29b) with boundary conditions given by Eqs. (29c) and (29d), we obtain

$$\frac{d\Phi_0}{d\eta} = \int_0^\eta \frac{u_*^2 + T_1}{\nu} d\eta_1 + \int_{-\infty}^{+\infty} \Delta U(K, \eta) dK, \quad (30)$$

where

$$\Delta U(K, \eta) = \left[\int_0^\eta \frac{\tau_{\text{wave}}(\eta_1)}{\nu} d\eta_1 + \int_{-\infty}^{+\infty} F_0(K) K^2 (\exp(-2K\eta) X_0 - \exp(-K\eta) \text{Re} X_2) dK \right] (1 + 2y_{1\gamma})$$

is the component added to the profile of the average-velocity and to its long-wavelength perturbation due to momentum transfer from a wind wave with wavenumber K to the wind flow.

With allowance for definition (23) of the function Φ it is not difficult to find the relationship between $U^{(1)} = d\varphi^{(1)}/d\eta$ (see Eq. (21)) and $d\Phi_0/d\eta$:

$$\frac{d\Phi_0}{d\eta} = U^{(1)} - 2\text{Re}[kac \exp(i\Sigma)] + U_0(\eta).$$

It is known that the coefficient ν of eddy viscosity has the linear asymptotic $\nu = 0.4u_*\eta$ [17] as the distance from the surface increases. In particular, this is obvious from Eq. (7)). At the same time, $\nu \rightarrow \nu_a = \text{const}$ for $\eta \rightarrow 0$. As a result, it is easily seen that the first term in Eq. (30) has a logarithmic asymptotic, and the second term tends to a certain constant:

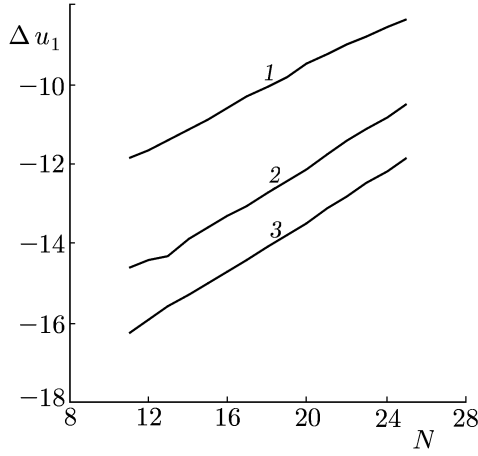


Fig. 1. Dependence of the parameter Δu_1 on the wind-wave "age" for the wind friction velocity $u_* = 10, 20,$ and 30 cm/s (curves 1–3, respectively).

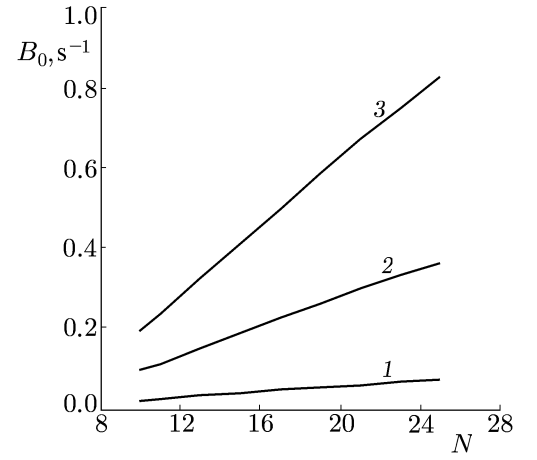


Fig. 2. Dependence of the growth rate of the wind waves with wavelength 2.3 cm on the wind-wave "age" for the wind friction velocity $u_* = 10, 20,$ and 30 cm/s (curves 1–3, respectively).

$$U_0(\eta) + U^{(1)} = \frac{u_*}{\kappa} \left[1 + \operatorname{Re} \left(\frac{T_1}{u_*^2} \exp(i\Sigma) \right) \right] \ln \frac{\eta}{\eta_0} + 2ck \operatorname{Re}[a \exp(i\Sigma)] + \int_{-\infty}^{+\infty} \Delta U(K, \eta) \Big|_{\eta \rightarrow \infty} dK,$$

where η_0 is the roughness parameter. For a hydrodynamically smooth flow, we have $\eta_0 = 0.118 \nu_a / u_*$. If the coefficient of turbulent-stress modulation is large, i.e., $m_T = |T_1 / (u_*^2 ka)| \gg 1$, then the transformation of short waves is mainly determined by the modulation of this quantity, and the terms of the order of $y_{1\gamma}$ in system of Eqs. (28) and (29) are negligible. Then, introducing the notation $\varepsilon = \operatorname{Re}[T_1 \exp(i\Sigma)] / u_*^2$, we arrive at

$$\nu X_0 \Big|_{\eta \rightarrow \infty} = u_*^2 (1 + \varepsilon) \Big|_{\varepsilon = \operatorname{Re}[kam_T \exp(i\Sigma)]},$$

and the formulas for U_0 and $U^{(1)}$ reduce to

$$U_0(\eta) = \frac{u_*}{\kappa} \ln \frac{\eta}{\eta_0} + \left(\int_{-\infty}^{+\infty} \Delta U(K, \eta) \Big|_{\eta \rightarrow \infty} dK \right) \Big|_{\varepsilon=0},$$

$$U^{(1)} = \left[\frac{u_*}{\kappa} \ln \frac{\eta}{\eta_0} + \left(\frac{\partial}{\partial \varepsilon} \int_{-\infty}^{+\infty} \Delta U(K, \eta) \Big|_{\eta \rightarrow \infty} dK \right) \Big|_{\varepsilon=0} \right] \operatorname{Re}[kam_T \exp(i\Sigma)]. \quad (31)$$

A comparison of Eqs. (31) and (21) yields

$$T_1 = \frac{2\kappa c u_* ka}{\ln \left(\frac{3.15 k c \nu_a}{\kappa u_*^2} \eta_0^+ \right) - \kappa \Delta u_1 + \pi i / 2}, \quad (32)$$

where

$$\Delta u_1 = \frac{1}{u_*} \frac{\partial}{\partial \varepsilon} \int_{-\infty}^{+\infty} \Delta U(K, \eta) \Big|_{\eta \rightarrow \infty} dK, \quad \eta_a^+ = \eta_0 u_* / \nu_a.$$

The first terms in the denominator of Eq. (32) is negative, so that the phase of the coefficient of turbulent-stress modulation is close to $-\pi$ in the linear approximation (for $\Delta u_1 < 0$) with respect to the wind-wave amplitude. The second term is positive since the change of the average velocity profile, resulting from the

nonlinear interaction with wind-wave field, is negative: $\Delta u_1 < 0$ (see [21]). This means that the phase T_1 can change if the absolute value of $\Delta u_1 < 0$ is sufficiently large.

To find Δu_1 , we solve numerically the self-consistent quasi-linear system of equations comprising the equations for the harmonics and for the average flow. The equations for each harmonic are solved numerically by a mesh method based on the Gauss elimination procedure adapted for a banded matrix.

Calculation of the modulated short-wave spectrum within the framework of the relaxation model requires knowledge of the quantities β_r and $B = (\delta B_0 / \delta u_*) u_*$, which enter Eq. (5), and Δu_1 . Within the framework of the quasi-linear model, these quantities are determined by the wind velocity and the wind-wave spectrum. In the calculations, we used the ‘‘JONSWAP’’ spectrum [25]

$$F_0(K) = \frac{1}{2} \alpha_p K^{-3} \exp \left[-\frac{5}{4} \left(\frac{K_p}{K} \right)^2 \right] \gamma^r, \quad (33)$$

$$r = \exp \left[-\frac{1}{2} \left(\sqrt{K} - \sqrt{K_p} \right)^2 / \left(\sigma \sqrt{K_p} \right)^2 \right],$$

where $\alpha_p = 0.57 (C_p / u_*)^{-3/2}$, $\gamma = 3.3$, $\sigma = 0.1$, $K_p = g / C_p^2$, $C_p = N u_*$ is the phase velocity of the energy-carrying component, N is the so-called parameter of the wind-wave ‘‘age,’’ and g is the free-fall acceleration. It is known that N increases with increasing fetch. It is well known [25] that the average slope of the wind-wave spectrum decreases with increasing N . Hence, the waves become ‘‘more linear.’’ The dependences of the problem parameters Δu_1 , $B_0 = \beta_r / 2$, and $B = (\delta B_0 / \delta u_*) u_*$ on the parameter N for several values of the wind friction velocity are presented in Figs. 1–3. It is seen in Fig. 1 that small values of N (‘‘young’’ wind waves) correspond to large moduli of the negative term added to the average velocity profile due to the nonlinear interaction between the wind waves and the wind flow. Evidently, this is inferred by the fact that smaller values of N correspond to larger average amplitudes of the wind-wave field. The wind growth rate B_0 of a short surface wave decreases with decreasing N (see Fig. 2) since the average wind velocity described by the quantity Δu_1 decreases.

The results of calculations of the hydrodynamical MTF are presented in Fig. 4 for conditions corresponding to the measurements [26]. The wavelength of the Bragg wave amounts to 2.3 cm, which correspond to the X radio-wave band. The theoretical curves are parameterized by the ‘‘age’’ of wind waves in the ‘‘JONSWAP.’’ The ‘‘age’’ parameter describes the degree of nonlinearity of the wind-wave field. Figure 4a shows the results of calculations of the hydrodynamical MTF for wind waves with infinitesimally small amplitudes. A comparison of Figs. 4b and 4c with Fig. 4a shows that the values of the MTF modulus, yielded by both the linear and quasi-linear theory, agree satisfactorily with experimental data given in [26]. However, the values of the phase calculated using the linear approximation contradict the experimental data (see Fig. 4a), while the quasi-linear approximation yields the values of the phase of the hydrodynamical MTF, which are in much better agreement with the experimental data (Figs. 4b and 4c).

The same figures show the values of the hydrodynamical MTF calculated without taking the effect of modulation of the Bragg-wave growth rate into account (see the dashed lines). It is seen that such calculations poorly agree with the measured values of the MTF phase and amplitude.

5. MODULATION OF SHORT SURFACE WAVES IN THE PRESENCE OF INTENSE INTERNAL WAVES

In this section, we present a model of centimeter-wave modulation in a field of intense internal waves.

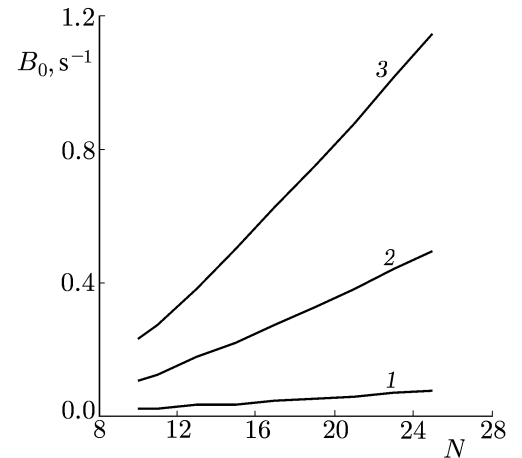


Fig. 3. Dependence of the parameter $B = (\partial B_0 / \partial u_*) u_*$ for a wave with wavelength 2.3 cm on the wind-wave ‘‘age’’ of for the wind friction velocity $u_* = 10, 20$, and 30 cm/s (curves 1–3, respectively).

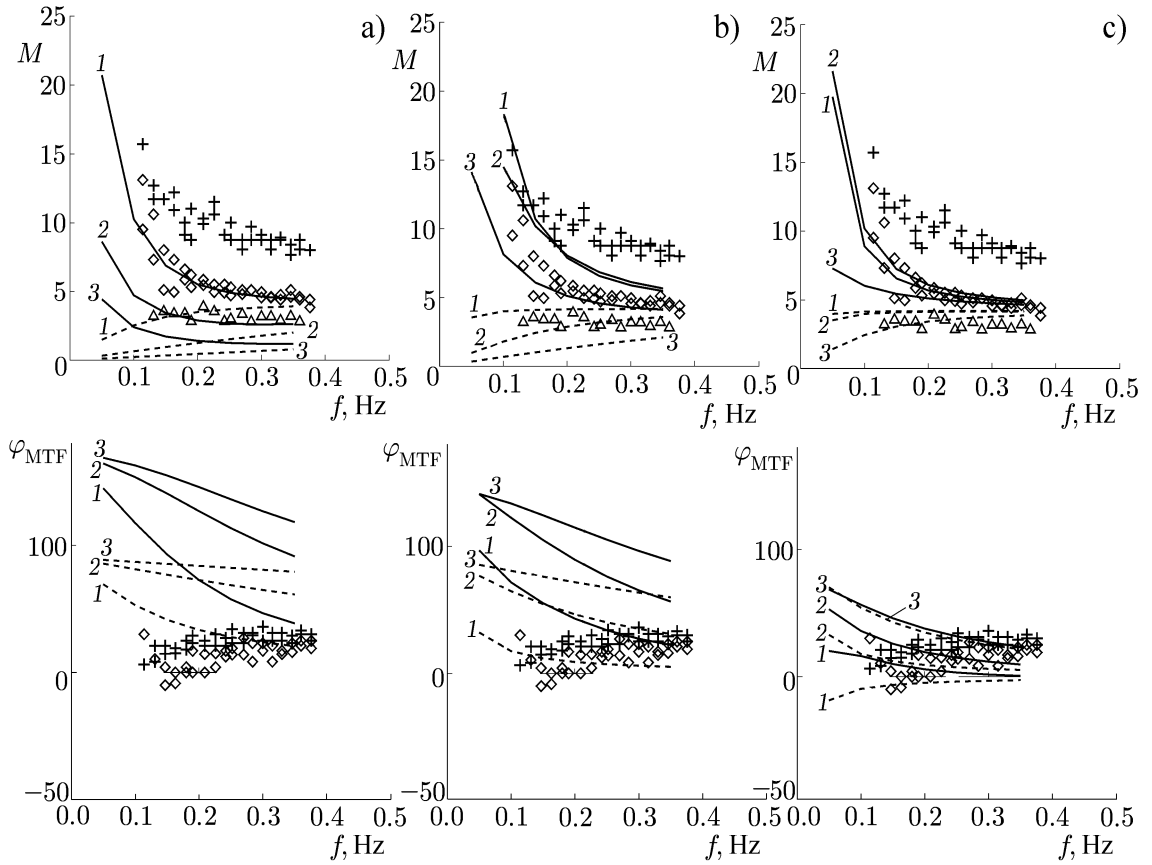


Fig. 4. Dependences of the quantity M and the phase φ_{MTF} of the hydrodynamical MTF on the frequency of the long-wavelength wave, calculated within the framework of the linear (a) and quasi-linear (b and c) theory. The short wavelength is equal to 2.3 cm. The solid lines correspond to the calculations with allowance for the growth-rate modulation, and the dashed lines, to the calculations without account of this effect. Curves 1 correspond to a wind friction velocity of 16 cm/s, curves 2, to 30 cm/s, and curves 3, to 50 cm/s. The experimental points are taken from [26]. The fetch parameter $N = 25$ (b) and $N = 10$ (c)

The internal-wave parameters are taken from the “COPE” experiment [11] in which superintense internal waves corresponding to high contrasts of the scattered radar signal were observed. The latter was probably stipulated by the high hydrodynamical contrast in the field of resonance centimeter surface waves. The results of this section are presented in [10] in greater detail.

To describe the flow field on a water surface generated by internal waves, we apply the Gardner model proposed in [27, 28].

5.1. Model of intense internal waves

The “COPE” experiment was aimed at studying flows generated powerful internal tides [11]. The observed picture showed the decay of a tidal wave in the shelf zone into a sequence of mutually interacting pulses propagated toward the coast. A number of features pointed out that the observed process was strongly nonlinear. In particular, the pulse amplitudes were several times larger than the thickness of the upper layer of water, and the pulse velocities were much larger (several times larger) than the velocity of long linear internal waves. A comparison made recently in [27, 28] showed that, in general, the evolution of large groups of such pulses can be adequately modelled by ensembles of interacting solitons within the framework of the combined Korteweg–de Vries equation with quadratic and cubic nonlinearities (the Gardner model):

$$\frac{\partial \eta}{\partial t} + c \frac{\partial \eta}{\partial x} + \alpha \eta \frac{\partial \eta}{\partial x} + \alpha_1 \eta^2 \frac{\partial \eta}{\partial x} + \beta \frac{\partial^3 \eta}{\partial x^3} = 0. \quad (34)$$

If the simplest two-layer model of the stratification is used, then the coefficients in Eq. (34) take the following values: $c^2 = gh_1 \Delta \rho / \rho$, $\alpha = 3c / (2h_1)$, $\beta = ch_1 h_2 / 6$, $\alpha_1 = -3c / (8h_1^2)$ (the mean values of the quantities h_1 , h_2 , and $\Delta \rho / \rho$ in the areas where the experiment was performed were $h_1 = 7$ m, $h_2 = 143$ m, $\Delta \rho / \rho = 3 \cdot 10^{-3}$). Equation (34) which is usually applied for a description of the evolution of weakly nonlinear long internal waves can be derived from the full system of hydrodynamical equations assuming that the deviation $\eta(x, t)$ of the interface between two liquids is small compared with the thicknesses h_1 and h_2 of the two layers and that the typical scales of internal waves are much larger than the total depth of the liquid. Moreover, the quadratic and cubic terms in Eq. (34) are usually kept simultaneously if the quadratic term is anomalously small, i.e., for $h_2 \approx h_1$. In this respect, it is important to emphasize that taking the nonlinear terms into account also in the case where $h_2 \gg h_1$, for which the approximation of weak nonlinearity is formally invalid, allows one to achieve a plausibly good correspondence between the amplitudes and velocities of the most intense observed pulses and the solitons of Eq. (34). Moreover, it was shown in [27] that the dynamics of interaction of the solitons is also very similar to the experimentally observed processes of collision of the pulses.

The behavior of ensembles comprising N interacting solitary waves is described in the so-called N -soliton solutions of completely integrable evolution equations to which Eq. (34) also belongs. However, the known formulas for the N -soliton solutions are so cumbersome and complicated, that it is difficult to retrieve detailed information on the interaction process, including the possibility of determination of the soliton parameters (such as its coordinate, velocity, and amplitude) at any time, directly from these formulas. The soliton interaction can be described in the simpler and much clearer way using an approximate approach familiar by its analogy with the description of collision of classical (point) particles [28, 29]. It was shown in [28] namely on the example of Eq. (34) that the approximate approach, even in the first order, can be improved such that the correct general structure of the exact N -soliton solution in the form of a rigorous superposition of quasi-solitons with relatively slowly varying parameters can be found. In this case, the solutions for the quasi-soliton parameters are determinative and remain qualitatively valid for arbitrary conditions of the problem, while higher-order approximations only refine these solutions.

The one-soliton solution of Eq. (34) has the form

$$\eta_s = \frac{\alpha}{2\alpha_1} \sqrt{\frac{V}{V_{\text{cr}}}} \left[\text{th} \frac{x - (c + V)t + \Delta}{2\sqrt{6\alpha_1\beta/\alpha^2}} - \text{th} \frac{x - (c + V)t - \Delta}{2\sqrt{6\alpha_1\beta/\alpha^2}} \right], \quad (35)$$

where $V_{\text{cr}} = \alpha^2 / (6\alpha_1)$, $\Delta \sqrt{V/\beta} = \text{Arch}(1/\sqrt{1 - V/V_{\text{cr}}})$. The amplitude

$$(\eta_s)_{\text{max}} = \frac{\alpha}{\alpha_1} \sqrt{\frac{V}{V_{\text{cr}}}} \text{th} \left(\Delta / \sqrt{6\alpha_1\beta/\alpha^2} \right)$$

of soliton (35) varies from zero, which corresponds to the soliton velocity equal to c , to the maximum value equal to α/α_1 , for which the soliton velocity is $c + V_{\text{cr}}$. Note that the most intense pulses of internal waves, observed in the ‘‘COPE’’ experiment, correspond namely to solitons close to the limiting ones.

The possibility of presenting soliton (2) in the form of a compound structure formed by more elementary formations, called kinks, is principal for the problem of the interaction of pulses. Such solutions exist within the framework of Eq. (34) for $V = V_{\text{cr}}$ and have the form

$$\eta_{\text{K}}^+ = \frac{\alpha}{2\alpha_1} \left(1 + \text{th} \left[\frac{x - (c + V_{\text{cr}})t}{2\sqrt{6\alpha_1\beta/\alpha^2}} \right] \right), \quad \eta_{\text{K}}^- = \frac{\alpha}{2\alpha_1} \left(1 - \text{th} \left[\frac{x - (c + V_{\text{cr}})t}{2\sqrt{6\alpha_1\beta/\alpha^2}} \right] \right). \quad (36)$$

A comparison of Eqs. (36) and (35) for $V \approx V_{\text{cr}}$, when the soliton has the form of a large-size plateau with

$\Delta \gg 1$, bounded by steep jumps of the field, makes it possible to write the solution of Eq. (35) in the following form:

$$\eta_s = \eta_K^+ + \eta_K^- - \frac{\alpha}{2\alpha_1} \approx \frac{\alpha}{2\alpha_1} \left[\text{th} \frac{x - (c + V_{\text{cr}})t + \Delta}{2\sqrt{6\alpha_1\beta/\alpha^2}} - \text{th} \frac{x - (c + V_{\text{cr}})t - \Delta}{2\sqrt{6\alpha_1\beta/\alpha^2}} \right]. \quad (37)$$

Equation (37) corresponds to a compound solution obtained by the method of matched asymptotic expansions [28]. Namely, the general solution is the sum of the solutions corresponding to the regions of strong variations in the field minus their common asymptotic being the solution in the external region. In the case considered, this asymptotic is simply the constant $\alpha/(2\alpha_1)$. The representation given by Eq. (37), which follows from the procedure of matching, does not yield all the soliton parameters (in particular, the quantity Δ), but reproduces correctly the overall structure of the field as the superposition of kinks. This allows one to search the solution of the more general problem of interaction of N solitons in the zero approximation as a superposition of $2N$ alternating kinks (36):

$$\eta_N^0(x, t) = \frac{\alpha}{2\alpha_1} \sum_{i=1}^{2N} (-1)^{i+1} \text{th} \frac{x - (c + V_{\text{cr}})t - S_i(t)}{2\sqrt{6\alpha_1\beta/\alpha^2}}. \quad (38)$$

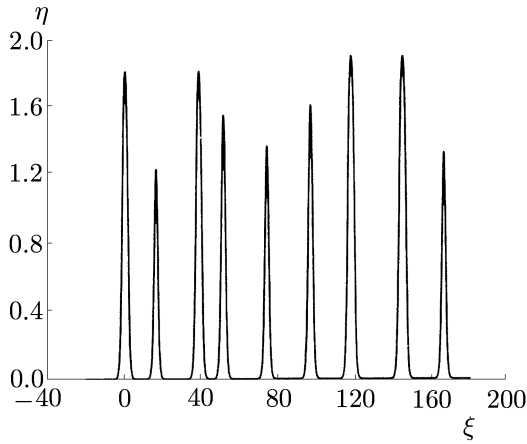


Fig. 5. Dependence of the isopycn displacement in the internal wave on the horizontal coordinate $\xi = x/L_x$.

Here, $S_i(t)$ is the slowly varying component of the coordinate of the i th kink, for which $dS_i/dt \ll V_{\text{cr}}$. The ratios $(V_{\text{cr}} - V_i)/V_{\text{cr}}$, where V_i are the velocities of the unperturbed stationary solitons, are the small parameters ε_i of the problem. The quantities ε_i introduced in such a way are evidently less than unity for all possible values of V_i .

The algorithm for constructing solutions in the higher approximations consists in finding local corrections, sought independently in the vicinity of each kink, and subsequent matching of these corrections. In addition, within the framework of each n th approximation, the procedure of matching the local corrections $\eta_i^{(n)}$ found in the vicinity of the i th kink should take into account the asymptotics of the corresponding order, which decay exponentially with increasing distance from the centers of the neighboring kinks.

Following this algorithm, we obtain that the general N -soliton solution with allowance for the corrections of the first approximation, takes the form

$$\eta_N^{(0)} + \eta_N^{(1)} = \frac{\alpha}{2\alpha_1} \sum_{i=1}^{2N} (-1)^{i+1} \left(1 - \frac{dS_i}{dt} \right) \text{th} \frac{x - (c + V_{\text{cr}})t - S_i(t)}{2\sqrt{6\alpha_1\beta/\alpha^2}},$$

where the kink coordinates S_i are found by solving the system of equations

$$\frac{dS_i}{dt} = -8 \text{ch}(S_{i+1} - S_i).$$

Satisfactory agreement between the theoretical calculations and the experimental data allows us to use the theoretical model for determination of the velocity field on the surface of a liquid.

Below we give the approximate formula for calculating a 9-pulse group, i.e., internal-wave solitons corresponding to the ‘‘COPE’’ observations, for the above-mentioned parameters at the fixed time t_0 :

$$\begin{aligned}
\eta_9^0(x, t_0) = & 14.03 \{ \text{th}[(25.7)^{-1}(x + 38.5)] - \text{th}[(25.7)^{-1}(x - 38.5)] \\
& + \text{th}[(25.7)^{-1}(x - 395.6)] - \text{th}[(25.7)^{-1}(x - 432.9)] + \text{th}[(25.7)^{-1}(x - 946.7)] - \text{th}[(25.7)^{-1}(x - 1023.8)] \\
& + \text{th}[(25.7)^{-1}(x - 1286.1)] - \text{th}[(25.7)^{-1}(x - 1339.5)] + \text{th}[(25.7)^{-1}(x - 1871.28)] - \text{th}[(25.7)^{-1}(x - 1914.5)] \\
& + \text{th}[(25.7)^{-1}(x - 2442.4)] - \text{th}[(25.7)^{-1}(x - 2499.6)] + \text{th}[(25.7)^{-1}(x - 2977)] - \text{th}[(25.7)^{-1}(x - 3070.8)] \\
& + \text{th}[(25.7)^{-1}(x - 3669.9)] - \text{th}[(25.7)^{-1}(x - 3763.1)] + \text{th}[(25.7)^{-1}(x - 4246.9)] - \text{th}[(25.7)^{-1}(x - 4288.3)] \}.
\end{aligned} \tag{39}$$

Here, the displacement of the surface and the coordinates are in meters. In what follows, this formula is used to calculate the velocity field on the surface of a two-layer liquid.

The dependence of the isopycn displacement in an internal wave on the horizontal coordinate $\xi = x/L_x$, where $L_x = 25.7$ m, calculated using Eq. (39), is shown in Fig. 5.

With allowance for the two-layer approximation of the stratification, the “rigid lid” condition on the surface, and the shallow-water approximation, the condition

$$\partial_t(h_1 + \eta) + \partial_x[(h_1 + \eta)U] = 0$$

of mass conservation in each layer yields the relationship

$$U[\text{m/s}] = 0.45 \frac{\eta_9(\text{m})/7}{1 + \eta_9(\text{m})/7} \tag{40}$$

between the above-obtained solutions η_N and the velocity field $U(x, t)$ on the surface for the model parameters mentioned above.

Based on the obtained approximate calculations for a group of nine pulses, i.e., solitons of internal waves corresponding to the “COPE” observations, we retrieve the velocity field on the surface and then use the retrieved velocity field to calculate modulation of the spectral density of the short-wave height field.

5.2. Wind boundary layer above a water surface with nonuniform flow field

Similar to the case of interaction with ripple waves, we describe a wind boundary layer above a rough sea surface within the framework of the system of Eqs. (19a), (19b) and (11). However, in contrast to long surface waves, the displacement of a surface in internal waves is almost absent. Hence, the “long-wavelength” transformation of coordinates, introduced in Sec. 4, is not applied.

The form of equations for a large-scale flow is identical to Eq. (8) with allowance for the replacement $(s, \gamma) \rightarrow (x, z)$, but the right-hand side, similar to Eqs. (12a) and (12b) includes the term $\partial^2 \tau / \partial \gamma^2$, where τ is the wave momentum flux. This term is negligible for weak winds when the contribution of the wave momentum flux to the transfer in the wind turbulent boundary layer is small [30]. If the wind is strong, then the effect of the wave momentum flux can be taken into account by using the modified expression for the effective eddy viscosity [19] (see Eq. (7)).

With allowance for these assumptions, the system of equations describing large-scale perturbations is identical to Eq. (8) with allowance for the replacements $z \rightarrow \gamma$ and $x \rightarrow s$. Taking into account that the velocity field $U(s, t)$ is a stationary wave, i.e., $U = U(s - ct)$, we obtain the following system of stationary equations in the frame moving with the velocity c :

$$\frac{\partial \psi}{\partial \gamma} \frac{\partial \chi}{\partial s} - \frac{\partial \psi}{\partial s} \frac{\partial \chi}{\partial \gamma} = \Delta(\nu \chi) - 2 \frac{\partial^2 \nu}{\partial \gamma^2} \frac{\partial^2 \psi}{\partial s^2}, \quad \Delta \psi = \chi. \tag{41}$$

Boundary conditions (9), similar to Eqs. (10c) and (10d), become

$$\psi|_{\gamma=0} = 0, \quad \left. \frac{\partial \psi}{\partial \gamma} \right|_{\gamma=0} = U(s) - c. \tag{42}$$

As the distance from the surface increases, the velocity field tends to the unperturbed logarithmic profile, i.e.,

$$\left. \frac{\partial \psi}{\partial \gamma} \right|_{\gamma \rightarrow \infty} = \frac{u_*}{0.4} \ln \frac{\gamma}{\gamma_0} - c.$$

The estimates given in [10] show that long-wavelength perturbations induced in the air by internal waves can be analyzed in the linear approximation. Then the system of equations for the perturbations reads

$$(U_0(\gamma) - c) \frac{\partial \chi_1}{\partial s} - \frac{d^2 U_0}{d\gamma^2} \frac{\partial \psi_1}{\partial s} = \Delta(\nu(\gamma)\chi_1) - 2 \frac{d^2 \nu}{d\gamma^2} \frac{\partial^2 \psi_1}{\partial s^2}, \quad \Delta \psi_1 = \chi_1, \quad (43)$$

$$\psi_1|_{\gamma=0} = 0, \quad \left. \frac{\partial \psi_1}{\partial \gamma} \right|_{\gamma=0} = U(s), \quad \left. \frac{\partial \psi_1}{\partial \gamma} \right|_{\gamma \rightarrow \infty} = 0,$$

where $U_0(\gamma) = -c + \int_0^\gamma [u_*^2/\nu(z)] dz$. If $\nu(z)$ is given by Eq. (7), then the asymptotic

$$U_0(\gamma) = -c + (u_*/\kappa) \ln(\gamma/\gamma_0)$$

holds for $\gamma \rightarrow 0$.

Such equations can be solved using the numerical procedure described in [21] and adapted for a nonharmonic perturbation.

Let the solution of system (43) be sought in the form of the Fourier integral

$$\begin{Bmatrix} \chi_1 \\ \psi_1 \end{Bmatrix} = \int_{-\infty}^{+\infty} \begin{Bmatrix} \chi_{1k}(\gamma) \\ \psi_{1k}(\gamma) \end{Bmatrix} \exp(iks) dk.$$

Then χ_{1k} and ψ_{1k} obey the following system of equations and boundary conditions:

$$(U_0(\gamma) - c) \chi_{1k} - \frac{d^2 U_0}{d\gamma^2} \psi_{1k} = \frac{1}{ik} \left[\left(\frac{d^2}{d\gamma^2} - k^2 \right) (\nu(\gamma)\chi_{1k}) + 2 \frac{d^2 \nu}{d\gamma^2} k^2 \psi_{1k} \right],$$

$$\frac{d^2 \psi_{1k}}{d\gamma^2} - k^2 \psi_{1k} = \chi_{1k},$$

$$\psi_{1k}|_{\gamma=0} = 0, \quad \left. \frac{d\psi_{1k}}{d\gamma} \right|_{\gamma=0} = \hat{U}(k), \quad \psi_{1k}|_{\gamma \rightarrow \infty} = 0. \quad (44)$$

Here, $\hat{U}(k)$ is the Fourier image of $U(s)$.

The system of equations (44) for the k th harmonic was solved numerically. The numerical calculations showed that the form of the solution on scales about the viscous-sublayer thickness depends only slightly on k . In this case, upon calculating the inverse Fourier transform of the obtained solution, we can present the velocity field of the perturbation, induced in the air by the field of an internal wave, in the following form:

$$U(s, \gamma) = \frac{\partial \psi}{\partial \gamma} = U(s) \operatorname{Re} \left(\frac{d\psi_{1k}}{d\gamma} \right) + \frac{1}{\pi} \int_{-\infty}^{+\infty} \frac{U(s')}{s - s'} ds' \operatorname{Im} \left(\frac{d\psi_{1k}}{d\gamma} \right), \quad (45)$$

where ψ_{1k} is the solution of Eq. (44) with boundary condition $d\psi_{1k}/d\gamma = 1$ for an arbitrary, sufficiently small k .

Using Eq. (45), it is easy to calculate $\chi_\gamma = \partial^2 U / \partial \gamma^2$ and the vorticity field $\chi = \partial U / \partial \gamma$ induced by the wave, which enter Eq. (44).

5.3. Modulation of short wind waves in the field of a wind over a sea surface in the presence of an internal wave

Variation in the spectral energy density $F(K, x, t)$ of short surface waves is described by kinetic equation (1). Before proceeding to calculations of the function F , we estimate the terms in Eq. (1) for the internal- and surface-wave parameters typical of the problem considered. The term on the left-hand side, which describes the kinematic effects, is of the order of Fc/L_x , where c and L_x are the phase velocity ($c = 50$ cm/s) and the typical scale ($L_x \approx 25$ m) of an internal wave, respectively. Hence, $Fc/L_x \sim 2 \cdot 10^{-2}F$. The right-hand side of Eq. (1) describes the effects stipulated by generation of waves by the wind and by the nonlinear wave interaction. These effects balance each other for the centimeter surface waves [26], so the right-hand side of Eq. (1) can be estimated using the surface-wave growth rate [31] $\beta = (0.02 - 0.04)(u_*^2/C_f^2)\Omega - 2\nu_w K^2$, where $\nu_w = 0.01$ cm²/s is the kinematic viscosity of water. If the wavenumber of the short wave is $K = 3$ cm⁻¹, then $\Omega \sim 70$ s⁻¹ and $C_f \sim 23$ cm/s, so that we have $\beta \sim 1$ s⁻¹ for $u_* = 20$ cm/s and $\beta \sim 0.1$ s⁻¹ for $u_* = 10$ cm/s since such a wind friction velocity is close to the generation threshold. This implies that the left-hand side describing the kinematic effects in the field of short waves is small, and the modulation of short waves is mainly contributed by their growth-rate modulation.

To calculate the modulation of the short-wave growth rate in the presence of an internal wave, we use the system of equations for short waves in the presence of long waves. This system of equations is analogous to the one used in Sec. 4. In the linear approximation, the complex amplitudes of the harmonics of perturbations of the stream function ψ_2 and the vorticity χ_2 with wavenumber K obey the system of equations identical to Eq. (28) for $y_{1\gamma} = 0$ with allowance for the ansatz $\eta \rightarrow \gamma$:

$$\left[\left[\left(\Phi_{0\gamma} - \frac{\Omega}{K} \right) \chi_2 - \psi_2 \chi_{0\gamma} \right] iK - \left(\frac{d^2}{d\gamma^2} - K^2 \right) (\chi_2 \nu) \right] = -2\nu_{\gamma\gamma} \psi_2 K^2 - 2KA \exp(-K\gamma) \left[\left(\Phi_{0\gamma} - \frac{\Omega}{K} \right) \nu_\gamma \right]_\gamma, \quad (46)$$

$$\frac{d^2 \psi_2}{d\gamma^2} - K^2 \psi_2 = \chi_2 - 2KA \exp(-K\gamma) \chi_0.$$

The boundary conditions have the form

$$\psi_2|_{\gamma=0} = 0, \quad \psi_{2\gamma}|_{\gamma=0} = 2\Omega A. \quad (47)$$

In contrast to Eq. (28), $\Phi_{0\gamma}$ and X_0 can be obtained in explicit form: $\Phi_{0\gamma} = U_0(\gamma) + U(s, \gamma) - \Omega/K$, where $U(s, \gamma)$ is given by Eq. (45), $\chi_0 = \Phi_{0\gamma\gamma}$, and A is the amplitude of the short surface wave.

Since the kinematic effects in the considered parameter range are small in comparison with the effects due to the interaction with the wind, the dependences of the wavenumber K and the phase velocity C_f of a short surface wave on the phase of an internal wave can be neglected in system (46) and boundary conditions (47).

By solving the system of equations (46), we can find the wind growth rate of short waves according to the formula

$$\beta_w = \frac{\rho_a}{2\rho_w} \nu_a \left[-\frac{\text{Re}(\chi_{2\gamma} - K\chi_2)}{C_f K A} + 4K^2 \right]. \quad (48)$$

In this case, the total growth rate of a short wave modulated by an internal wave has the form

$$\beta = -2\nu_w K^2 + \beta_w.$$

The dependences of β on the wave phase are presented in Figs. 6a and 6b for the cases where an internal wave propagates downwind (Fig. 6a) and upwind (Fig. 6b). A comparison with Fig. 5, in which the isopycn displacement in the internal wave is plotted versus ξ , shows that the maximum of the displacement (and the horizontal velocity) coincides with the minimum of the downwind growth rate of wind waves

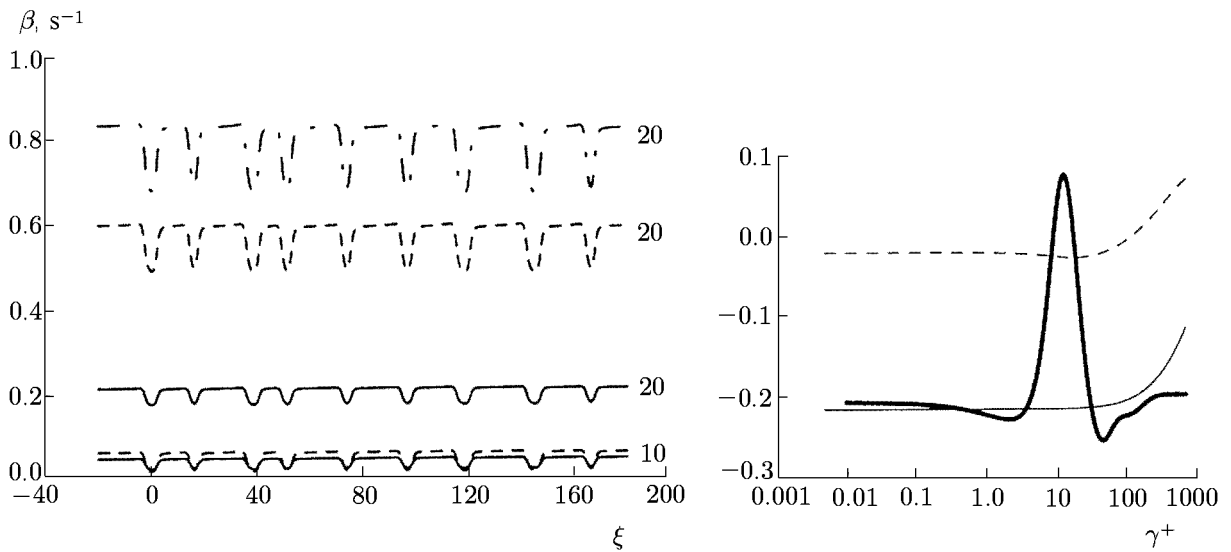


Fig. 6a. Dependences of the growth rate β on the horizontal coordinate $\xi = x/L_x$ ($L_x = 25.7$ m). The internal-wave phase velocity is directed downwind. The solid curves correspond to $K = 1 \text{ cm}^{-1}$, the dashed curves, to $K = 2 \text{ cm}^{-1}$, and the dash-dot curve, to $K = 3 \text{ cm}^{-1}$. The value of the wind friction velocity in cm/s is indicated near each curve. The right panel shows the plots of the real (solid curve) and imaginary (dashed curve) parts of the perturbation of the wind tangential stress, which is induced by a long harmonic wave. The thick curve is the power density of the energy exchange between the short wave and the wind (in relative units).

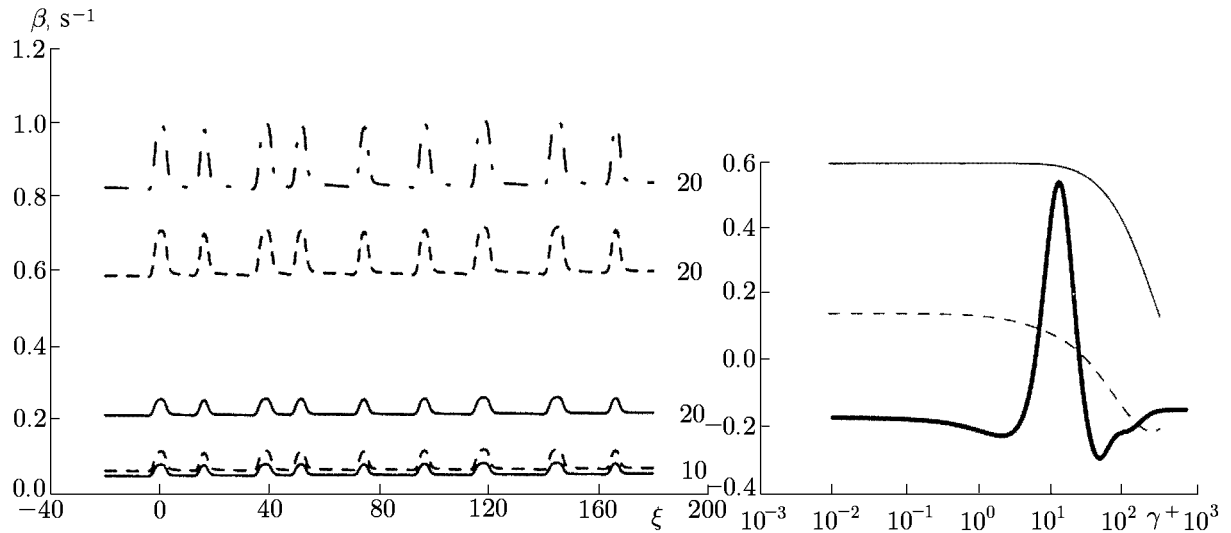


Fig. 6b. The same as in Fig. 6a, but in the case where the phase velocity of the internal wave is directed upwind.

(Fig. 6a) and with the maximum of the upwind growth rate of wind waves (Fig. 6b). To explain this effect, we also show in Fig. 6 the profiles of the real ($\text{Re } T_1$) and imaginary ($\text{Im } T_1$) parts of the perturbation of wind tangential stress induced by a harmonic wave with wavenumber $k = 0.25 \text{ m}^{-1}$. The same figure shows the profile of the power density of the radiative and viscous forces, averaged over the wave period, which determine the energy flux from the wind to the waves [22]. It is seen that the momentum-flux perturbations are almost constant in the region of the maximum energy exchange, and the phase of these perturbations is close to $-\pi$ and 0 downwind and upwind, respectively. Since T_1 does not depend on the vertical coordinate in the region where the energy exchange is significant, the formula

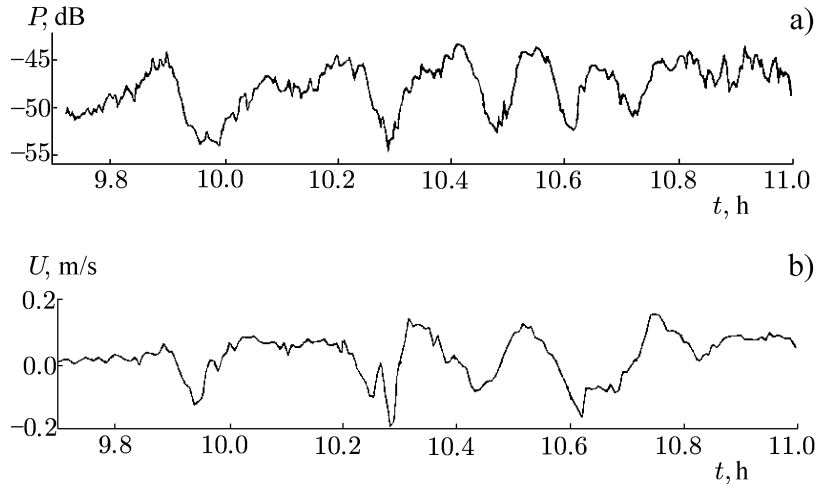


Fig. 7. Temporal dependences of the power of scattered radio signal (a) and the horizontal flux at a depth of 30 m (b) according to the data of [32].

$$U_0(z) = \left(\frac{u_*}{0.4} + \operatorname{Re} \frac{T_1 k a \exp(ikx)}{0.4 u_*^2} \right) \ln \frac{z}{z_0}$$

describes the wind velocity profile in this region with good accuracy.

Thus oscillations of the effective wind velocity are anti-phase with the velocity on the surface in the case of a tail wind and are in-phase in the case of a head wind. This effect has the simple physical explanation: the difference between the velocities on the surface and in the overlying layers of the wind boundary layer is less if a downwind flow exists on the surface, and the smaller velocity difference results in a smaller friction stress. If the wind and water-surface velocities are antiparallel, then the friction stress is much larger.

If the tangential-stress perturbation T_1 is almost constant in the region of energy exchange between a wind wave and an air flow, then the modulation of the wind growth rate is entirely determined by the modulation of T_1 . This explains the dependences $\beta(\xi)$.

Let us apply the results of the developed model to estimating the data of the “COPE” experiment in which the intensity of radio signal scattered from the sea surface and oscillations of the thermocline were simultaneously measured on the coastal shelf near the state of Oregon [32]. It was found that the minima of the scattered radio-signal power and the thermocline displacements were approximately in-phase. The same phase relationship holds between the modulated wind growth rate of short surface waves and the isopycn displacement of an internal wave propagated downwind (Fig. 6a).

To compare the experimental results with our model, we use the wind and wave parameters measured during the “COPE” experiment in September 23, 1995. Figure 7 presents the data on the under-thermocline horizontal velocity of the flow stipulated by internal waves and on the corresponding scattered-signal power. Note that the isopycn displacement is anti-phase to the the velocity of the under-thermocline flow, i.e., the scattered-signal minimum also coincides with the maximum of the isopycn displacement. In this case, the wind velocity amounts to 9.5 m/s ($u_* \approx 28.5$ cm/s), and the angle between the wind-velocity and wave-propagation directions, to $\theta \approx 60^\circ$. The velocity of internal-wave propagation was $c_{IW} = 1.03$ m/s. The measurements were performed using a radar with radiation wavelength $\lambda = 3$ cm at grazing angles, i.e., the

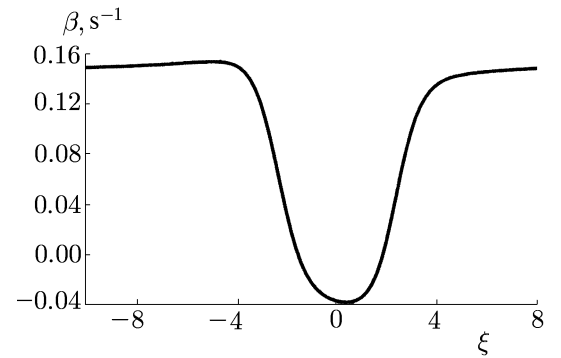


Fig. 8. Dependence of the modulated growth rate of a surface wave on the horizontal coordinate ξ . The wind and wave parameters correspond to the conditions of September 23, 1995 (according to the data [32]). The wavenumber of the surface wave is $K = 4 \text{ cm}^{-1}$.

Bragg wavelength was equal to 1.5 cm.

We calculated the modulated growth rate of Bragg waves within the framework of our model for the above-mentioned parameters. Note that the wind and wave velocities are assumed aligned in this model. Since the radar viewing direction was the same as the direction of internal-wave propagation, we adopted for estimates that the surface velocity in the internal wave is equal to $c_{IW} = 1.03$ m/s and the wind friction velocity amounts to $u_{*1} = u_* \cos \theta \approx 14.3$ cm/s. The calculated modulated growth rate is shown in Fig. 8. It is seen that the phase of the growth-rate modulation is opposite to the isopycn-displacement phase, and the growth rate even reverses sign at the isopycn-displacement maximum.

6. CONCLUSIONS

This paper is devoted to a description of one mechanism of modulation of short surface waves in the presence of nonuniform flows. It is well known that nonuniform flows on a water surface induce irregularities in the wind field, which, in turn, give rise to the irregularities of wind-ripple generation, i.e., to a modulation of the wind growth rate of surface waves. This mechanism was considered for the first time in the case where a nonuniform flow was induced by a long wave on a water surface [5]. However, development of the consistent theory of this mechanism of short-wave modulation encountered significant difficulties related, first and foremost, to determination of the phase of the surface-wave modulation coefficient, which was experimentally observed to be close to zero, while it appeared to be close to $-\pi$ in the theory. Taking into account the nonlinear effect of the wind-profile deformation in the presence of surface wave allows one to explain theoretically the values of both the amplitude and the phase of the modulation coefficient of the surface-wave spectrum.

The mechanism of surface-wave growth rate modulation turns out to be efficient also in the case where a nonuniform flow field on a surface is generated by intense internal waves. Note that the effect of growth-rate modulation is considered in this paper without account of the conservative kinematic transformation of surface waves. At the same time, modulation of short surface waves in a field of intense internal waves was studied earlier in [33] without allowance for the growth-rate modulation. It was shown in that paper that in the case of very short intense internal waves, a significant hydrodynamical contrast exists even for centimeter waves. Analyzing the combined influence of these two effects will be done elsewhere later on.

This work was supported by the Russian Foundation for Basic Research (project No. 02-05-65099) and the Council for Grants of the President of the Russian Federation for the Support of Leading Scientific Schools (grant No. NSh-1637.2003.2, the scientific school of V. I. Talanov).

REFERENCES

1. A. Ya. Basovich, V. V. Bakhanov, and V. I. Talanov, in: *Influence of Large-Scale Internal Waves on a Sea Surface*, Inst. Appl. Phys. Press, Gorky (1982), p. 8.
2. A. Ya. Basovich, V. V. Bakhanov, D. M. Bravo-Zhivotovsky, L. B. Gordeev, Yu. M. Zhidko, and S. I. Muyakshin, *Dokl. Akad. Nauk SSSR*, **298**, No. 4, 967 (1988).
3. S. A. Ermakov and S. G. Salashin, *Dokl. Akad. Nauk SSSR*, **337**, No. 1, 108 (1994).
4. M. G. Bulatov, Yu. A. Kravtsov, O. Yu. Lavrova, K. Ts. Litovchenko, M. I. Mityagina, M. D. Raev, K. D. Sabinin, Yu. G. Trokhimovskii, A. N. Churyumov, and I. V. Shugan, *Physics — Uspekhi* **46**, 63 (2003).
5. M. T. Landahl, S. E. Widnall, and L. Hultgen, *Proc. 12th Symp. on Naval Hydrodynamics.*, National Acad. Sci. (1978).
6. K. Hasselman, et al., *J. Geophys. Res.*, **90**, 4659 (1985).
7. S. A. Grodsky, V. N. Kudryavtsev, and V. K. Makin, *Morskoi Gidrofiz. Zh.*, No. 1, 15 (1991).

8. Yu. I. Troitskaya, “Modulation of the growth rate of a short surface wave excited by a turbulent wind in the presence of a long wave,” preprint No. 391 [in Russian], Inst. Appl. Phys. Press, Nizhny Novgorod (1996).
9. Yu. I. Troitskaya, “Quasi-linear model of the modulation of short surface waves excited by a turbulent wind in the presence of ripples,” preprint No. 544 [in Russian], Inst. Appl. Phys. Press, Nizhny Novgorod (2000).
10. K. A. Gorshkov, I. S. Dolina, I. A. Soustova, and Yu. I. Troitskaya, *Izvestiya, Atmos. Oceanic Phys.*, **39**, No. 5, 596 (2002).
11. T. P. Stanton and L. A. Ostrovsky, *Geophys. Rev. Lett.*, **25**, 2695 (1998).
12. M. S. Longuet-Higgins and R. W. Stewart, *J. Fluid Mech.*, **8**, No. 4, 565 (1960).
13. M. S. Longuet-Higgins and R. W. Stewart, *J. Fluid Mech.*, **10**, No. 4, 529 (1961).
14. M. S. Longuet-Higgins, *J. Fluid Mech.*, **177**, 293 (1987).
15. W. C. Keller and J. W. Wright, *Radio Sci.*, **10**, 139 (1975).
16. J. A. Smith, *Surface Waves and Fluxes, Vol. 1*, Kluwer Academic Publ. (1990), p. 247.
17. A. S. Monin and A. M. Yaglom, *Statistical Fluid Mechanics, Vol. 1*, MIT Press, Cambridge, Massachusetts (1971).
18. A. V. Smol’yakov, *Akust. Zh.*, **19**, No. 3, 420 (1973).
19. D. S. Riley, M. A. Donelan, and W. H. Hui, *Boundary Layer Meteor.*, **22**, 209 (1982).
20. A. D. Jenkins, *J. Phys. Oceanogr.*, **22**, No. 8, 843 (1992).
21. V. P. Reutov and Yu. I. Troitskaya, *Izv. Rossiisk. Akad. Nauk, Fiz. Atmos. Okeana*, **31**, No. 6, 623 (1995).
22. Yu. I. Troitskaya, *Izv. Rossiisk. Akad. Nauk, Fiz. Atmos. Okeana*, **33**, No. 4, 525 (1997).
23. *Reviews on Plasma Physics, Vol. 7* [in Russian], Énergoatomizdat, Moscow (1973).
24. T. Benjamin Brooke, *J. Fluid Mech.*, **6**, 161 (1959).
25. K. Hasselman, et al., *Dtsch. Hydrogr. Z. Reihe A*, **8**, 12 (1973).
26. W. Plant J., W. C. Keller, and A. Cross, *J. Geophys. Res.*, **88**, 9747 (1983).
27. K. A. Gorshkov, V. G. Irisov, L. A. Ostrovsky, and I. A. Soustova, “Multisoliton solutions of Gardner equation and their applications” (in press).
28. K. A. Gorshkov and I. A. Soustova, *Radiophys. Quantum Electron.*, **44**, Nos. 5–6, 465 (2001).
29. J. Grue and L. A. Ostrovsky, “Strongly nonlinear internal solitons — analytical models and fully nonlinear computations” (in press).
30. V. N. Kudryavtsev, C. Mastenbroek, and V. K. Makin, *Boundary Layer Meteor.*, **83**, 99 (1997).
31. W. Plant, *J. Geophys. Res.*, **87**, 1961 (1982).
32. R. A. Kropfli, et al., *J. Geophys. Res.*, **104**, 3133 (1999).
33. V. V. Bakhanov and L. A. Ostrovsky, “The action of strong solitary internal waves on surface waves,” preprint No. 573 [in Russian], Inst. Appl. Phys. Press, Nizhny Novgorod (2001).